Design and Test of a Nb_3Sn Subscale Dipole Magnet for Training Studies

Helene Felice, Shlomo Caspi, Daniel R. Dietderich, Paolo Ferracin, Steve A. Gourlay, Aurelio R. Hafalia, Alan F. Lietzke, Alain Mailfert, GianLuca Sabbi, Pierre Vedrine

***Abstract*—As part of a collaboration between CEA/Saclay and the Superconducting Magnet Group at LBNL, a subscale dipole structure has been developed to study training in Nb_3Sn coils under variable pre-stress conditions. This design is derived from the LBNL Subscale Magnet and relies on the use of identical Nb_3Sn racetrack coils. Whereas the original LBNL subscale magnet was in a dual bore "common-coil" configuration, the new subscale dipole magnet (SD) is assembled as a single bore dipole made of two superposed racetrack coils. The dipole is supported by a new mechanical structure developed to withstand the horizontal and axial Lorentz forces and capable of applying variable vertical, horizontal and axial preload. The magnet was tested at LBNL as part of a series of training studies aiming at understanding of the relation between pre-stress and magnet performance. Particular attention is given to the coil ends where the magnetic field peaks and stress conditions are the least understood. After a description of SD design, assembly, cool-down and tests results are reported and compared with the computations of the OPERA3D and ANSYS magnetic and mechanical models.**

***Index Terms*—dipole magnet, Nb_3Sn, training**

I. Introduction

UP to now, the use of pre-stress in Nb_3Sn magnets relies on knowledge gained with NbTi. Consequently, the mechanical structures are designed to maintain coils in compression during excitation. But due to the Nb_3Sn stress sensitivity, the pre-stress could become a threat for the superconducting properties of the coils. Indeed, by increasing the magnetic field, the Lorentz forces produced in coils become higher and the pre-stress necessary to prevent separation between the coil and the support structure has to be reinforced. So, there is a risk for high field magnets that the accumulation of stresses in the coils becomes larger than what is currently considered a safe limit of 150 MPa [1]. It is then legitimate to wonder what would be the influence of a low pre-stress on the training. It could be relevant to see if it is possible to decrease the pre-stress without preventing the magnet from reaching its short sample from current. Nevertheless, whatever the low preload tests results, it will remain necessary to understand the influence of large stresses on coils and to define the limit above it the Nb_3Sn superconducting properties are degraded.

To investigate these issues, the Subscale Dipole magnet SD has been developed. On one hand, it aims at understanding of the influence of low lateral and axial preload on training. On the other hand, it also permits the application of high pre-stress. In this paper, the general Subscale Dipole design is depicted as well as the parameters of SD01 (Subscale Dipole 01) which is the first magnet based on this concept. The first test of SD01 consists in validating the behavior of the mechanical structure. During this nominal test, the coils are supposed to be maintained in compression. The assembly, cool-down and tests results of SD01 in this nominal configuration are reported here.

Manuscript received August 29, 2006.

H. Felice and P. Vedrine are with CEA/Saclay, DAPNIA/SACM/LEAS, 91191 GIF-SUR-YVETTE CEDEX, FRANCE (phone: +33 1 69 08 57 56, fax : +33 1 69 08 92 83, e-mail: helene.felice@cea.fr).

A. Mailfert is with LEM, 54500 VANDOEUVRE, FRANCE

All the other authors are with Lawrence Berkeley National Laboratory, Berkeley, CA

II. Magnet Design

A. General concept

The Subscale Dipole SD has to fit three main requirements. It has to be representative of a dipole magnet, to allow variable vertical, horizontal and axial preloads and to be easy to handle. The dipolar magnetic configuration can be obtained by the use of two superposed racetrack coils. To make the assembly and disassembly easy, subscale coils have been chosen.

Regarding the application of the variable lateral pre-stress, the solution chosen relies on the key and bladders technology [2]. As the pre-stress has to be applied vertically and horizontally, the coil support structure comprises four pads. They are surrounded by two halves yoke and an outer aluminum shell (Fig. 1). All the parts are assembled with

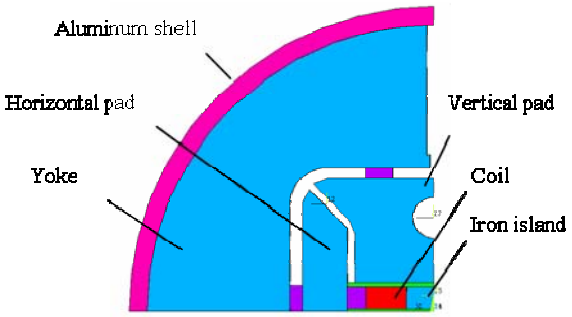

Fig. 1. SD01 magnet cross-section.

pressurized bladders and stainless steel keys. The axial preload is applied by means of two aluminum rods going through the vertical pads.

B. Magnetic Design

The design of the subscale dipole magnet consists of two "SC" type Subscale Coil modules: SC01 and SC02 (MJR strands [3]). The cable is composed of 20 Nb_3Sn strands with a diameter of 0.7 mm and is insulated with a 0.1 mm thick woven sleeve of fiberglass. Each "SC" module is a double-layer racetrack coil wound around an iron pole, reacted and epoxy impregnated. The main parameters of the conductor are

TABLE I
CONDUCTOR AND COIL PARAMETERS

	SC01	SC02	Units
Strand diameter	0.7	0.7	mm
Cu/nonCu ratio	0.87	0.87	
Manufacturer	OST	OST	
Type	MJR	MJR	
Jc @ 12T 4.2K	2334	2334	
RRR	38	37	
Cable width	7.938	7.938	mm
Cable thickness	1.280	1.280	mm
Number strands	20	20	
Insulation thickness	0.1	0.1	mm
Number layer s per coil	2	2	
Number turns per layer	20	20	

listed in Table I.

The superposition of SC01 and SC02 gives a dipolar field which peaks in the coil ends. The difference between the field in the ends and the field in the centre of the straight section is equal to 2.7 T. To decrease this value, it has been decided to keep iron only in the central part of the magnet to reinforce the magnetic field in the straight section. That is why the yoke has a 101,6 mm iron central part and the vertical pad has a 110 mm iron central part. Nevertheless, to insure a homogeneous horizontal pre-stress, the horizontal pad is kept in one iron piece. In this configuration, the peak field is still located in the coil ends but the difference between the field in the ends and in the centre of the straight section has been lowered to 1T. The short sample value has been obtained by the intersection between the critical curve measured at LBNL on SC01 and SC02 strand and the magnet load line computed with OPERA3D (Fig. 2). The expected performance parameters of the magnet are reported in Table II.

C. Mechanical Design

As mentioned before, the main components of the support structure are: two horizontal iron pads, two vertical pads, a two halves yoke, and an outer aluminum shell. Both the vertical pads and the yoke are split into three parts, with a central one in iron and outer parts in stainless steel. At room temperature, once the coil package is positioned in the yoke with nominal keys, bladders are introduced between pads and yoke. The pressurization of the bladders creates gaps between yoke and nominal keys which are filled by interference keys. When the expected pre-stress is reached, the bladders are deflated and removed. The coil package is then pre-

TABLE II
PERFORMANCES PARAMETERS

	Symbol	Quantity	Units
Short sample current	I_{ss}	8750	A
Coil peak field @ I_{ss}	B_{PF}	12.45	T
Axial Lorentz forces per coil @ I_{ss}	F_z	84.8	kN
Horizontal Lorentz force per coil @ I_{ss}	F_x	291	kN
Vertical Lorentz force per coil @ I_{ss}	F_y	-238	kN

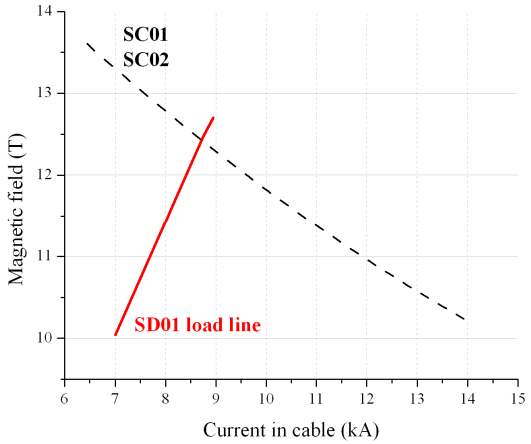

Fig. 2. Measurements of the magnetic field versus critical current at 4.2K for the conductor of SC01 and SC02 (dashed line) and computed load line for SD01 (solid line).

compressed by the nominal keys and interference keys stack. During the cool-down, due to the different thermal contraction of aluminum and iron, the shell shrinkage increases the lateral preload on the coil package.

Regarding the axial preload, a longitudinal support system which has already been carried out in the HD1 magnet [4], in the SQ magnet [5], and in the TQ magnet [6] has been included in the design. Two aluminum rods, with a diameter of 24 mm are inserted in the holes of the vertical pads and bolted to two 57 mm thick stainless steel end plates (Fig. 3). The rods are pre-tensioned at room temperature with an axial piston to provide a first axial compression on the coils. During the cool-down, the rods shrinkage increases the axial preload.

The mechanical behavior of the magnet has been analyzed with a 3D finite element model implemented in the ANSYS code. Several cases have been considered with different friction coefficients. In this paper, the numerical results matching the experimental results are presented: a friction of

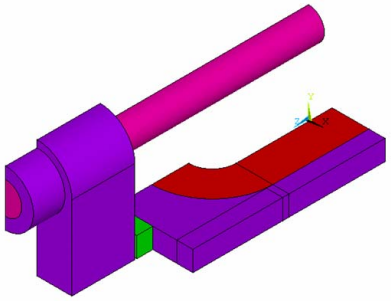

Fig. 3. An aluminum rod bolted to a stainless steel end plate applies axial preload on the subscale racetrack coil.

0.1 has been assumed between all surfaces except between the yoke and the shell where a frictionless behavior has been

exhibited during assembly. The results of the numerical computation for the stress in the coil in the straight section and in the ends are depicted in Fig. 4. The graph shows the horizontal stress in the coil straight section on the island side $\sigma_{X\ coil\ ss}$ and the axial stress in the coil end on the island side $\sigma_{Z\ coil\ end}$ during assembly (Rods and Bladders in Fig. 4), cool-down (4.2 K in Fig. 4) and as a function of a fraction of the Lorentz forces (I^2/I_{ss}^2 in Fig. 4). During excitation at the short sample, the stresses in the coil end and in the coil straight section have the same order of magnitude. These values were chosen high enough to ensure contact between coil and island with a safety margin. Indeed, the model predicts a margin of 36 MPa in the straight section and a margin of 35 MPa in the ends.

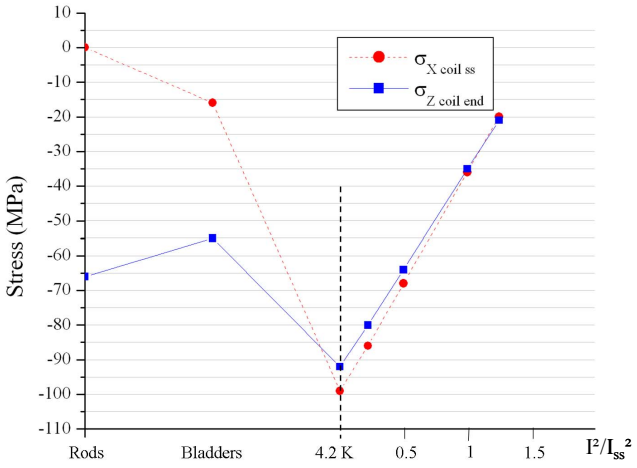

Fig. 4. Computed stress variation in the coil on the island side in the straight section and in the end in MPa during assembly, cool-down and excitation.

III. Assembly and Cool-Down

A. Assembly

The outer shell has been instrumented with four strain gauges. All of them are distributed on both sides of the magnet mid plane. On each side, the azimuthal and the axial strains are measured. The measurements of the shell strain performed during the assembly are plotted in Fig. 5. Two additional strain gauges are attached to the aluminum rods to measure their axial tension. Target strains are computed by the ANSYS model and the assembly is completed when these strain targets are reached. In SD01 case, it corresponds to an azimuthal strain of around 460.10^{-6} (460 με) in the shell (32 MPa) and an axial strain of 1220 με in the rods (105 MPa).

Since in previous magnets the axial preload provided by the rods shrinkage during cool-down was observed to be smaller than the value expected by ANSYS computation, a higher axial preload (about 1570 με) had to be applied at room temperature in order to reach the target value after cool-down (2400 με) and to ensure the expected compression during excitation.

During assembly, a significant spring back, maybe caused by some misalignment of the parts in the structure, has been exhibited after the key insertion: as shown in Fig. 5, a pressure of 28 MPa (4000 psi) was needed to insert a key stack equivalent to 14 MPa (2000 psi).

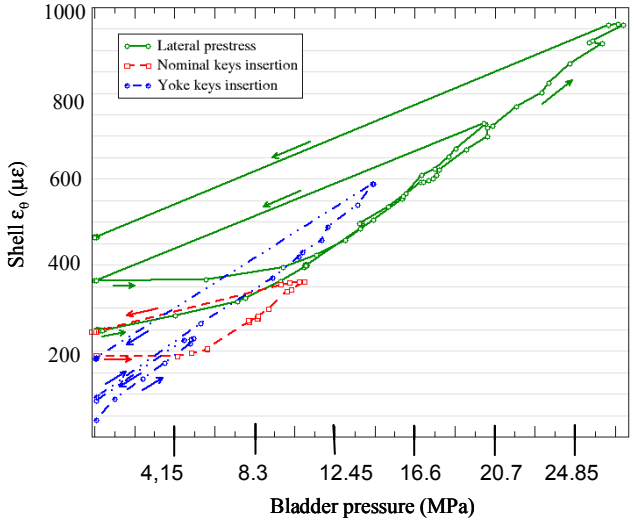

Fig. 5. Measured azimuthal strain variation in the shell in με during assembly versus bladders pressure in MPa: during yoke positioning (dot dash line), during coil package nominal positioning in the yoke (dash line), during axial preload (solid line).

B. Cool-down

During cool-down, the shrinkage of the shell and of the rods provides additional pre-stress on the coil. The variation of the strain in the shell and in the rods during cool down is depicted in Fig. 6. From zero to 20 hours, the cool-down is provided by LN. Then LN is replaced by LHe. This explains the change of behavior of the parts around 20 hours. The strains measured by mean of the strain gauges on the shell (Fig. 6-(a) and 6-(b)) and on the rods (Fig. 6-(c)) can be compared to the values expected with the ANSYS model. In SD01 case, the azimuthal strain was supposed to reach a strain of 1631 με (136 MPa) after cool-down in the shell and the final strain measured was

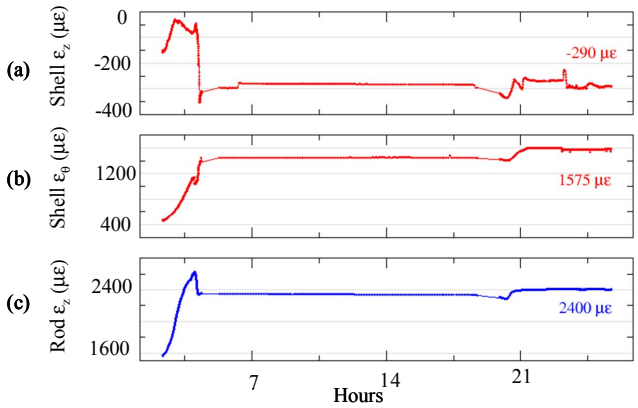

Fig. 6. (a) Measured axial strain variation in the shell – (b) Measured azimuthal strain variation in the shell – (c) Measured axial strain variation in the rods during cool-down versus time in hours.

equal to 1575 με (133 MPa). In the axial direction, due to the frictionless hypothesis the axial strain was supposed to be equal to one third of the azimuthal one that is to say around – 500 με. The measurement gives – 290 με, showing a higher friction than at room temperature. Regarding the rods, their tensile strain increased during cool-down from 1570 (113

MPa) to 2400 με (192 MPa) as it was expected. In addition, Fig. 6 shows a high growth of the tensile strain of the rod during the first hours of cool-down followed by a steep decrease. This is due to the fact that at the beginning of the cool-down, the rods are cooled faster and shrink a lot compared to the other parts. After few hours, the contraction of all the other components determines a decrease of rod tension.

IV. Tests Results

Test of SD01 carried out at 4.3 K (complete quench history shown in Fig. 7) included 11 training quenches, 11 ramp-rate quenches and 5 additional quenches at variable ramp-rates (40 A/s then 5 A/s, 80 A/s then 5 A/s, 150 then 80 then 5 A/s).

A. Training Quenches

The current ramp-rate of the two first quenches was equal to 20 A/s. The first training quench occurred at 8556 A which corresponds to 98% of the expected short sample current of the magnet (8750 A). From the third to the last training quench, the same current ramp was used and was equal to 20 A/s to 8000 A and 5 A/s to quench. The highest current (8953 A) was reached on the fifth attempts after which an erratic plateau was exhibited around the expected short sample current. The 2% discrepancy between the expected short sample current and the measured maximum current remains in

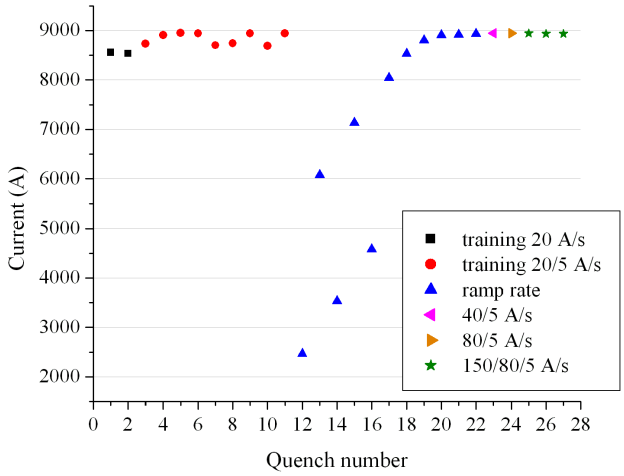

Fig. 7. SD01 quench history.

the uncertainties of the critical current measurement. All the training quenches occurred in SC02.

B. Ramp-rate Dependence

Eleven ramp-rate quenches were performed from 600 A/s to 1 A/s. Currents reached during this study are reported in Fig. 7 and 8. All but 4 quenches occurred in SC02. The linear variation of the quench current versus the ramp-rate seems to indicate that the dominant phenomenon involved is the losses due to filaments magnetization. The large size of the filament (70 microns) and a comparison of the order of magnitude of the different kind of losses confirm this hypothesis.

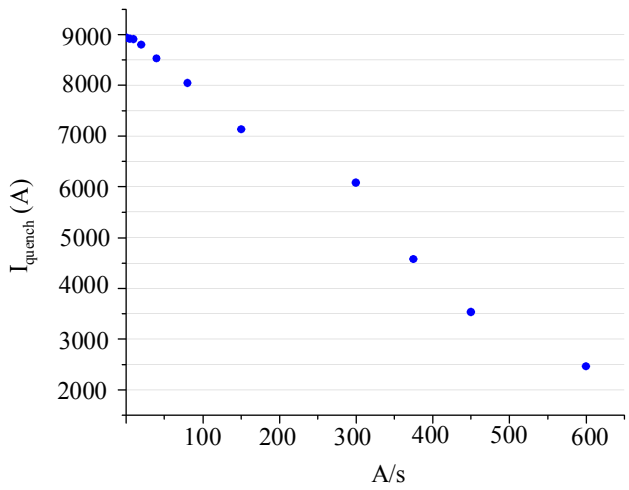

Fig. 8. SD01 ramp rate dependence.

After the ramp-rate study, 5 additional quenches have been performed with variable current ramp profiles (40 A/s to 8 kA and 5 A/s to quench, 80 A/s to 8 kA and 5 A/s to quench, 150 to 6.8 kA, 80 A/s to 7.8 kA and 5 A/s to quench). These five quenches have an onset typical of short sample conditions and their currents were above 8934 A. This result shows that the current ramp profile does not affect the magnet performances if the ramp is slowed early enough to allow the removal of the heat produced by the losses.

C. Strain Gauges Measurements

The goal of the pre-load procedure applied in this first test was to minimize the structure motion during excitation. Indeed, if the pre-stress applied by the keys stack is high enough, the Lorentz forces are compensated. That means that the strain in the shell remains constant during excitation. It was the case during SD01 training as shown on Fig 9-(b). It can be concluded that the horizontal preload applied was

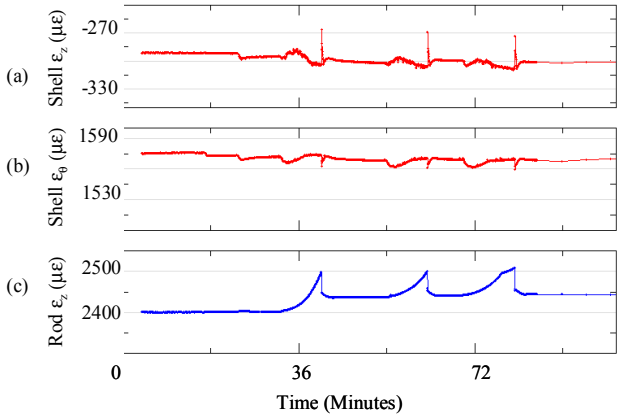

Fig. 9. (a) Measured axial strain variation in the shell – (b) Measured azimuthal strain variation in the shell – (c) Measured axial strain variation in the rods during training versus time in minutes.

sufficient to prevent the separation of the coil from the pole and to ensure contact between the coils and the mechanical structure.

Regarding the measurements of the strain on the axial rods (Fig. 9-(c)), they show that the tension in the rods increases slightly (few MPa) during excitation because of the axial Lorentz forces growth. This stress increase is plotted on Fig.

10 as a function of a fraction of the Lorentz forces in the magnet and compared to the ANSYS computation. It appears that the measured rods response is slightly higher than expected, indicating a very low friction coefficient between coil and structure. As the coils have already been tested in several magnetic configurations, some degree of freedom

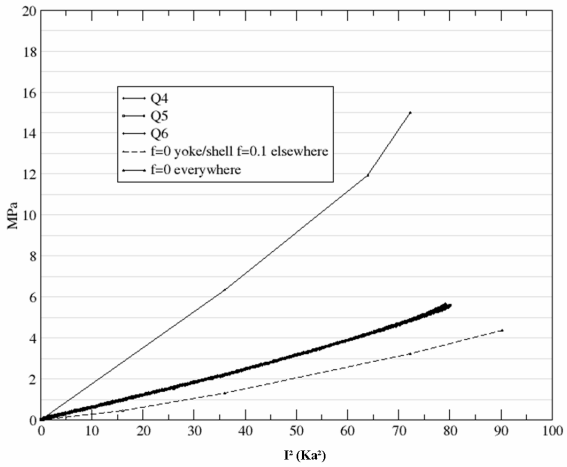

Fig. 10. Measured and computed stress variation in the rods during excitation.

could have been released between the island and the coils. Moreover, a small phenomenon of ratcheting (few με), which has already been noticed in previous magnets [7], has been observed (Fig. 9-(c)). It consists in a cumulative residual deformation of the structure in the axial direction. Most of the residual deformation is usually observed during the first loading cycle, which is confirmed by SD01 test with a strain increase from 2400 με to 2436 με.

V. Perspectives

SD01 has shown a reliable mechanical structure. This encouraging result shows that pre-stress studies can be performed. On one hand, studies can be made by focusing on the ends behavior where the field peaks. On the other hand, the coil design can be improved to move the peak field in the straight section. This can be achieved by the introduction of a spacer in the ends. It seems possible to introduce this spacer without major change in the tooling. For instance, a 10 mm spacer in coils with bronze island should allow a 0.6 T higher field in the straight section. With this new kind of coils, stresses limit could be investigated because peak field and stresses could coincide in the straight section.

From the modeling viewpoint, this study confirms that the friction coefficient is a key parameter for the understanding of the mechanical structure behavior. Some uncertainties remain here regarding the value of the coefficient to take into account to match as well as possible the experimental results. This understanding could be helped by a better instrumentation of the structure and of the coils for the next tests.

VI. Conclusion

A Nb_3Sn subscale dipole magnet SD01 has been designed, and fabricated in collaboration between CEA/Saclay and LBNL and has been tested at LBNL. The magnet relies on subscale racetrack coils arranged for the first time in a dipole configuration. SD01 had a first quench at 98% of the expected short sample and 96% of the maximum current reached. The mechanical structure exhibited a reliable behavior, with strain measurements close to the expected values. Now that it has been validated, the SD structure can allow low and high pre-stress studies.

References

[1] E. Barzi, "Superconductor and cable R&D for High Field Accelerator Magnets at Fermilab", invited paper at the international Workshop on Progress of Nb-based Superconductors, Feb. 2-3, 2004.

[2] S. Caspi et al., "The use of pressurized bladders for stress control of superconducting magnets", *IEEE Trans. Appl. Supercond*., vol. 11, no. 1, pp 2272-2275, March 2001.

[3] W.K. McDonald et al., "Manufacture and evaluation of Nb_3Sn conductors fabricated by the MJR method", *IEEE Trans. Magn.*, vol. MAG-19, no. 3, pp 1410-1416, May 1983.

[4] A.R.Hafalia et al., "HD1: Design and Fabrication of a 16 T Nb_3Sn Dipole Magnet", *IEEE Trans. Appl. Supercond.,* vol.14, no.2, pp 283-286, June 2004.

[5] P. Ferracin et al., "Assembly and test of SQ01b, a Nb_3Sn Quadrupole Magnet for the LHC Accelerator Research Program", *IEEE Trans. Appl. Supercond.,* vol. 16, no.2, pp 382-385, June 2006.

[6] S. Caspi et al., "Design and Analysis of TQS01, a 90 mm Nb_3Sn Model Quadrupole for LHC Luminosity Upgrade Based on Key and Bladder Assembly", *IEEE Trans. Appl. Supercond.*, vol. 16, no. 2, pp 358-361, June 2006.

[7] S. Mattafirri et al., "Performance Analysis of HD1 : A 16 Tesla Nb_3Sn Dipole Magnet", *IEEE Trans. Appl. Supercond*., vol. 15, no. 2, pp 1156, June 2005.